Prepared by F.L. Lewis and E. Stingu
Updated: Saturday, November 12, 2022

Potential Fields in Cooperative Motion Control and Formations

Add discussion. Refer to refs.

1.1 Potential Fields

Equation Chapter 1 Section 1

The potential is a scalar field whose negative gradient is a vector field of conservative forces. Consider a planar field of play having some targets and some obstacles. A sample 2-D playing field is shown in Figure 1.1-1. The targets or goals are endowed with attractive potentials and the obstacles with repulsive potentials. From the potentials, one computes the associated forces. At any point (x, y) in the plane, the sum of forces at that point gives a net force produced by all the targets and all the obstacles. The net force as a function of position is a vector force field that represents the resultant force obtained by summing the effects of the attraction force of the target and the repulsion forces of the obstacles

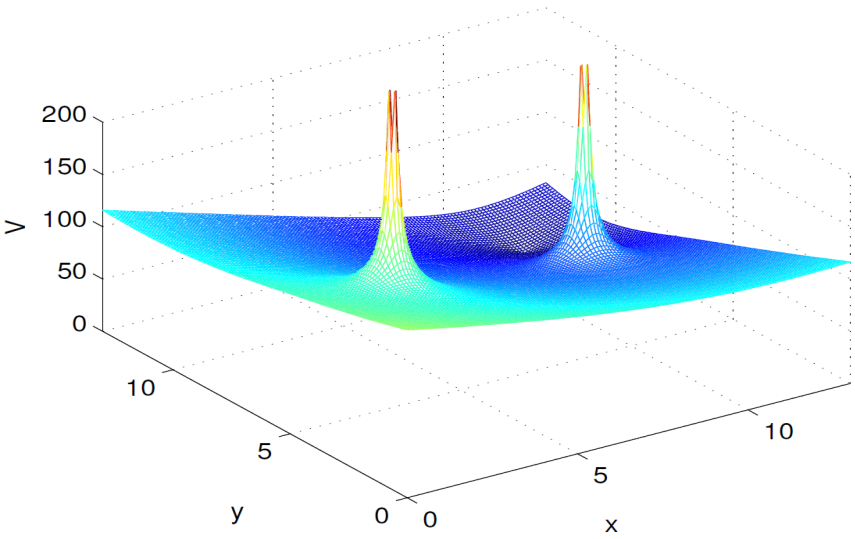


Fig. 1.1-1. Sample 2-D playing field for vehicle motion control

$$\vec{F}(\vec{r}) = \vec{F}_{target}(\vec{r}) + \sum_{i=1}^{n} \vec{F}_{obs_i}(\vec{r}) = -\vec{\nabla} V(\vec{r}) \tag{1.1.1}$$

where arrows denotes vectors. In potential field motion control, it is important to keep track of forces, their components, and their directions. For mobile ground robot applications, the potential fields are usually used in a 2-dimensional space. Then $\vec{r} = \begin{bmatrix} x & y \end{bmatrix}^T \in R^2$ and the force gradient is

$$\vec{\nabla} V(\vec{r}) = \begin{bmatrix} \frac{\partial V}{\partial x} & \frac{\partial V}{\partial y} \end{bmatrix}^T = \begin{bmatrix} F_x & F_y \end{bmatrix}^T \in R^2 \tag{1.1.2}$$

with x and y components

$$F_x(x,y) = -\frac{\partial V(x,y)}{\partial x}$$
$$F_y(x,y) = -\frac{\partial V(x,y)}{\partial y} \tag{1.1.3}$$

The trajectory of motion of a ground robot is generated continuously for any position (x, y) of the robot by following the direction of the steepest descent in the potential field, since that is the direction of the net force at that point. This can be considered an optimization problem that searches for the point of minimum potential.

Some sample potential fields and the forces they generate are given now. Suppose it is desired to reach a target located at (x_1, y_1) and the current vehicle position is $(x(t), y(t))$. A linear attractive potential is

$$V(r) = kr \tag{1.1.4}$$

where the distance to the target is $r = [(x - x_1)^2 + (y - y_1)^2]^{1/2}$. Then by the chain rule the gradient force generated is

$$F_x = -\frac{\partial V}{\partial x} = -k\,\tfrac{1}{2}[(x - x_1)^2 + (y - y_1)^2]^{-1/2}\,2(x - x_1) = k\frac{(x_1 - x)}{r} \tag{1.1.5}$$

$$F_y = -\frac{\partial V}{\partial y} = -k\,\tfrac{1}{2}[(x - x_1)^2 + (y - y_1)^2]^{-1/2}\,2(y - y_1) = k\frac{(y_1 - y)}{r} \tag{1.1.6}$$

Note that

$$e_x = \frac{(x - x_1)}{r}, \quad e_y = \frac{(y - y_1)}{r} \tag{1.1.7}$$

are the components of a unit vector and so the attractive force is constant independent of the distance to the target. This means that the attractive effects of the target have an unbounded range of influence.

Suppose, on the other hand, that it is desired to avoid an obstacle located at (x_1, y_1) and the current vehicle position is $(x(t), y(t))$. A repulsive potential is

$$V(r) = \frac{k}{r} \tag{1.1.8}$$

where the distance to the obstacle is $r = [(x - x_1)^2 + (y - y_1)^2]^{1/2}$. Then by the chain rule the gradient force generated is

$$F_x = -\frac{\partial V}{\partial x} = -k\frac{\partial r^{-1}}{\partial x} = -k(-r^{-2})\,\tfrac{1}{2}[(x - x_1)^2 + (y - y_1)^2]^{-1/2}\,2(x - x_1) = -\frac{k}{r^2}\frac{(x_1 - x)}{r} \tag{1.1.9}$$

$$F_y = -\frac{\partial V}{\partial y} = -k\frac{\partial r^{-1}}{\partial y} = -k(-r^{-2})\,\tfrac{1}{2}[(x - x_1)^2 + (y - y_1)^2]^{-1/2}\,2(y - y_1) = -\frac{k}{r^2}\frac{(y_1 - y)}{r} \tag{1.1.10}$$

Note that

$$e_x = \frac{(x - x_1)}{r}, \quad e_y = \frac{(y - y_1)}{r} \tag{1.1.11}$$

are the components of a unit vector and so the force follows a repulsive square law. This is

similar to the electrostatic force or gravitational force and means that the repulsive effects of the obstacles have a limited range of influence.

Sample potential fields are shown in Figure 1.1-2. Shown is an environment on the square [0,12]x[0,12] in the (x, y) plane with a goal or target at $(x_G, y_G) = (10,10)$ and obstacles at $(x_1, y_1) = (3,3)$, $(x_2, y_2) = (7,2)$.

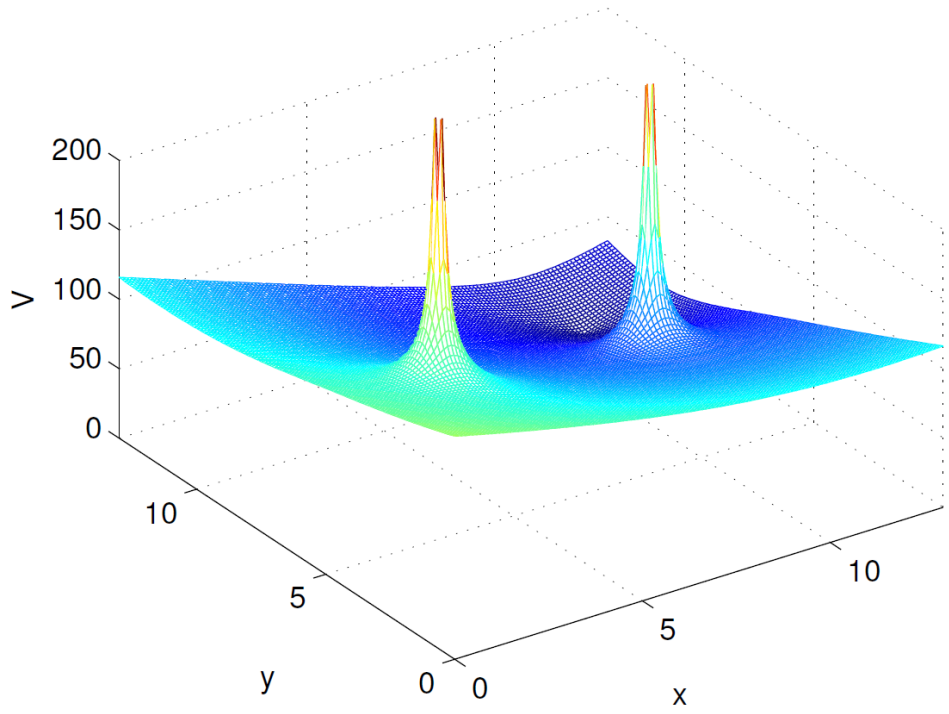


Fig. 1.1-2. Potential Fields for target and two obstacles.

1.2 Potential Fields for Vehicle Control

Equation Section (Next)

Consider the model of a car-like vehicle. This is a nonholonomic system, so it can only turn with a finite turn radius. Thus, it may not be able to follow the ideal trajectory resulting from the potential field. However, the potential field implicitly provides a feedback mechanism. That is, the force $\vec{F}$ is generated for any position of the robot in such a way that it will return close to the ideal trajectory.

Vehicle Dynamics

The robot vehicle shown in Figure 1.2-1 has the dynamics

$$\dot{x} = v_T \cos\phi \cos\theta$$
$$\dot{y} = v_T \cos\phi \sin\theta \qquad (1.2.1)$$
$$\dot{\theta} = \frac{v_T}{L}\sin\phi$$

with (x, y) the position, θ the heading angle, v_T the forward wheel speed, L the wheel base, and ϕ the steering angle. In this model, the control input is the steering angle $\phi(t)$.

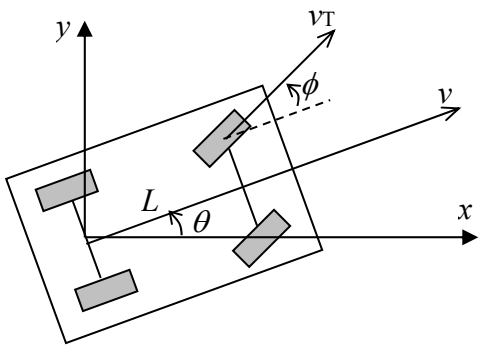


Figure 1.2-1. Model of a car-like robot

A simplified model of a vehicle is given by

$$\dot{x} = v_T \cos\theta$$
$$\dot{y} = v_T \sin\theta \qquad (1.2.2)$$

In this model, the control input is the heading angle $\theta(t)$. Either model can be used for simulation depending on the degree of accuracy to real life wanted.

Generating the Potential Fields

Consider the environment on the square [0,12]x[0,12] in the (x, y) plane shown in Figure 1.1-2 with a goal or target at $(x_G, y_G) = (10,10)$ and obstacles at $(x_1, y_1) = (3,3)$, $(x_2, y_2) = (7,2)$. The potential fields for motion towards the goal while avoiding the two obstacles are generated as follows.

The target potential field (1.1.4) yields a constant force independent of distance that attracts the robot to the target. The attractive force when the vehicle is at position (x, y) is defined in terms of the range to the target

$$r_G = \sqrt{(x_G - x)^2 + (y_G - y)^2} \qquad (1.2.3)$$

as

$$F_{Gx}(x, y) = K_G \frac{x_G - x}{r_G}, \qquad F_{Gy}(x, y) = K_G \frac{y_G - y}{r_G} \qquad (1.2.4)$$

Computing the obstacle forces based on the potential field (1.1.8) yields the repulsive square law forces

$$F_{ix}(x, y) = -K_i \frac{x_i - x}{r_i^2} \qquad (1.2.5)$$

$$F_{iy}(x, y) = -K_i \frac{y_i - y}{r_i^2} \qquad (1.2.6)$$

where $r_i = \sqrt{(x_i - x)^2 + (y_i - y)^2}$ is the distance between the robot and the i-th obstacle.

There are many other methods for computing potential forces for repulsion and attraction. For example, assuming the obstacles are circular, the force for the i-th obstacle can be taken as

$$F_{ix}(x,y) = -K_i \frac{x_i - x}{\left(\max\left\{(r_i - a_i), b_i\right\}\right)^2}, \quad F_{iy}(x,y) = -K_i \frac{y_i - y}{\left(\max\left\{(r_i - a_i), b_i\right\}\right)^2}, \tag{1.2.7}$$

where a_i is the radius of the i-th obstacle and b_i limits the relative height of the i-th obstacle potential field.

The total force that acts on the robot is

$$\begin{aligned} F_x &= F_{Gx} + F_{1x} + F_{2x} \\ F_y &= F_{Gy} + F_{1y} + F_{2y} \end{aligned} \tag{1.2.8}$$

The angle of the force indicates the desired direction of motion of the vehicle. The angle of the force as seen from the robot is

$$\alpha = \tan^{-1}\left(\frac{F_y}{F_x}\right) \tag{1.2.9}$$

Feedback Control System for Potential Field Motion

The angle of the summed forces is interpreted as a desired heading angle $\theta_{des} = \alpha$ for the vehicle. To follow this angle one can design the feedback control system shown in Figure 1.2-2. The

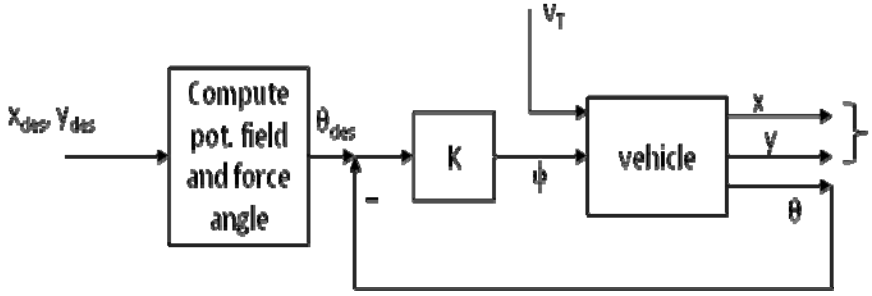


Fig. 1.2-2. Feedback system for vehicle motion control

control input to the vehicle is the steering angle $\phi(t)$. The speed v_T can be kept constant, or reduced as one approaches near an obstacle.

A simulation is now performed. The initial position for the robot is $(x_0, y_0) = (0,0)$ and the initial heading angle is $\phi_0 = \frac{\pi}{6}$ rad. The speed v_T is kept constant. The steering angle is generated by the controller based on the difference between the heading angle θ and the angle α of the resultant force acting on the robot (Fig. 2). In this example, a

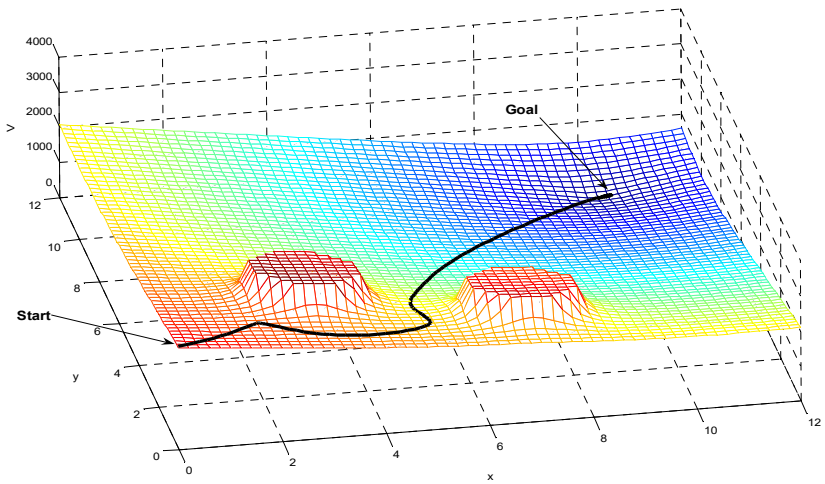


Figure 1.2-3. The trajectory of the robot using potential fields

proportional controller is implemented:

$$\varphi = K(\alpha - \theta)$$

The resulting motion is shown in Figure 1.2-3, along with the potential fields generated. In this simulation, the potential fields corresponding to (1.2.7) are used.

Problems with Potential Field Methods

It can be seen from the potential field representation that the robot will follow the direction of the steepest descent, which is the direction of the resultant force. There are a few issues that can prevent the robot to reach the target.

The sum of forces is equal to zero at any point (x, y) where the net potential has a local minimum. At these points, the vehicle will stop. One situation where this can occur is if there are obstacles spaced too close together. The vehicle will attempt to pass between the obstacles due to the attractive force towards the target, but will not be able to pass between the obstacles. Such problems can be solved by adding a dither to the force which results in small random motions that can help get out of local minima. Alternatively, one can modify the height or dimension of the obstacle potential fields, or change the type of force used to represent them, or use an intelligent controller in the outer loops of controller shown in Figure 1.2-2.

Another problem arises with nonholonomic vehicles. These vehicles have a finite turning radius and cannot make arbitrarily tight turns. If the vehicle misses the target by a small amount, it will try to turn towards the target. If the attractive force generates a desired heading direction that cannot be reached with the vehicle's turn radius, the vehicle will circle the target and never reach it.

1.3 The Graph Laplacian Potential and Gradient-Based Cooperative Control

Equation Section (Next)

In this section we study a potential function that is naturally associated with a graph, the Graph Laplacian Potential, and show how to use it to generate local cooperative control protocols.

Graph Laplacian Potential

Consider a dynamic graph $G = (V, A)$ with N nodes $v_i \in V$, the state of i-th node given by x_i, and connectivity matrix $A = [a_{ij}]$. The in-degree is the i-th row sum of A $d_i = \sum_j a_{ij}$. The graph Laplacian is $L = D - A$ with $D = diag[d_i]$. Define $x = [x_1 \cdots x_N]^T$, with $x_i(t)$ a state associated with each node i.

The graph Laplacian potential

$$V_G = \sum_{i,j} a_{ij}(x_j - x_i)^2 \tag{1.3.1}$$

is a measure of the energy stored in the graph. Clearly

$$V_G = \sum_{i,j} a_{ij}(x_j - x_i)^2 \geq 0\,. \tag{1.3.2}$$

The Laplacian potential is useful in cooperative control on any graph, including general digraphs. The next result shows that it takes a special form for undirected graphs.

Lemma 1.3-1. Let the graph be undirected. Then

$$V_G = \tfrac{1}{2}\sum_{i,j} a_{ij}(x_j - x_i)^2 = x^T L x \tag{1.3.3}$$

Proof:

$$2V_G = \sum_{i,j} a_{ij}(x_j - x_i)^2 = \sum_j x_j \sum_i a_{ij}(x_j - x_i) - \sum_i x_i \sum_j a_{ij}(x_j - x_i)$$

First term on the right is

$$\sum_j x_j \sum_i a_{ij}(x_j - x_i) = \sum_j x_j^2 \sum_i a_{ij} - \sum_j x_j \sum_i a_{ij} x_i$$

Interchange index variables in first term here to get

$$\sum_j x_j \sum_i a_{ij}(x_j - x_i) = \sum_i x_i^2 \sum_j a_{ji} - \sum_i \sum_j a_{ij} x_i x_j$$

However, the *i*-th row sum $\sum_j a_{ij}$ (in-degree) is equal to the *i*-th column sum $\sum_j a_{ji}$ (out-degree) if the graph is undirected. Therefore,

$$\sum_j x_j \sum_i a_{ij}(x_j - x_i) = \sum_i x_i^2 \sum_j a_{ij} - \sum_i \sum_j a_{ij} x_i x_j = -\sum_i x_i \sum_j a_{ij}(x_j - x_i)$$

and

$$2V_G = \sum_{i,j} a_{ij}(x_j - x_i)^2 = 2\sum_j x_j^2 d_i - 2\sum_j x_j \sum_i a_{ij} x_i = 2x^T L x \qquad \blacksquare$$

This result shows that for undirected graphs the Laplacian matrix is positive semi-definite $L \geq 0$. For general digraphs it is not possible to express the graph potential V_G in terms of the Laplacian matrix, and the definition of V_G must be modified. This issue is studied in a subsequent chapter. The next exercise shows that for balanced graphs the potential as defined in (1.3.1) also has a special form in terms of the Laplacian matrix.

Exercise 1.3-1. Laplacian Potential for Balanced Graphs. The *i*-th row sum $\sum_j a_{ij}$ (in-degree) is equal to the *i*-th column sum $\sum_j a_{ji}$ (out-degree) if and only if the graph is balanced. Show that for balanced graphs

$$V_G = \tfrac{1}{2}\sum_{i,j} a_{ij}(x_j - x_i)^2 = \tfrac{1}{2} x^T (L + L^T) x \tag{1.3.4}$$

This proves that for balanced graphs $(L + L^T)$ is positive semidefinite. $\blacksquare$

Gradient-Based Control for First-Order Scalar Dynamics

Consider a general directed graph with agent motion in 1-D along the line and the agent dynamics

$$\dot{x}_i = u_i \tag{1.3.5}$$

with $x_i, u_i \in R$. Select the control input given by the gradient of the Laplacian potential as

$$u_i = -\frac{\partial V_G(x)}{\partial x_i} = \sum_j a_{ij}(x_j - x_i) = \sum_{j \in N_i} a_{ij}(x_j - x_i) \tag{1.3.6}$$

This is the standard local voting protocol we have analyzed at length. Note that sums over *j* can be taken as sums over the neighbor set N_i of *i* since only for these values of *j* are $a_{ij} \neq 0$.

In terms of the global control $u = [u_1 \cdots u_N]^T \in R^N$ and state one has

$$u = -Lx \tag{1.3.7}$$

$$\dot{x} = -Lx \tag{1.3.8}$$

It is interesting to note that the global dynamics of the agents is given in terms of the Laplacian matrix for any graph even though, for general digraphs, the identity (1.3.3) does not hold.

First-Order Motion Dynamics in the 2-D Plane

Consider now motion in the (x, y) with velocity control dynamics (1.3.5) and states $x_i = [p_i \;\; q_i]^T \in R^2$ where $(p_i(t), q_i(t))$ is the position of node *i* in the (x, y)-plane. Now the Laplacian potential is

$$V_G = \tfrac{1}{2}\sum_{i,j} a_{ij}(x_j - x_i)^T(x_j - x_i) = \tfrac{1}{2}\sum_{i,j} a_{ij} r_{ij}^2 \tag{1.3.9}$$

where the distance between nodes *i* and *j* is

$$r_{ij} = \sqrt{(p_j - p_i)^2 + (q_j - q_i)^2} \tag{1.3.10}$$

Compute the gradients to get the forces in the *x* and *y* directions as

$$\frac{\partial V_G}{\partial p_i} = \sum_j a_{ij} r_{ij} \frac{\partial r_{ij}}{\partial p_i} = -\sum_{j \in N_i} a_{ij}(p_j - p_i) \tag{1.3.11}$$

$$\frac{\partial V_G}{\partial q_i} = \sum_j a_{ij} r_{ij} \frac{\partial r_{ij}}{\partial q_i} = -\sum_{j \in N_i} a_{ij}(q_j - q_i) \tag{1.3.12}$$

The gradient-based control now gives the *x* and *y* velocity inputs

$$u_{pi} = -\frac{\partial V_G}{\partial p_i} = \sum_{j \in N_i} a_{ij}(p_j - p_i) \tag{1.3.13}$$

$$u_{qi} = -\frac{\partial V_G}{\partial q_i} = \sum_{j \in N_i} a_{ij}(q_j - q_i) \tag{1.3.14}$$

That is, for 2-D motion systems (1.3.5) one takes independent standard local voting protocols in each component of the motion *x* and *y*. The *x* and *y* motion protocols may be combined to write

$$u_i = -\frac{\partial V_G}{\partial x_i} = \sum_{j \in N_i} a_{ij}(x_j - x_i) \tag{1.3.15}$$

where $x_i, u_i \in R^2$.

Note that this situation of first-order motion dynamics in the 2-D (x,y)-plane is not the same as second-order consensus considered in Chapter 2. Second-order consensus takes the dynamics for coupled systems that satisfy Newton's law $\ddot{x}_i = u_i$, which yields the second-order node dynamics

$$\begin{aligned} \dot{x}_i &= v_i \\ \dot{v}_i &= u_i \end{aligned} \tag{1.3.16}$$

with position $x_i \in R$, velocity $v_i \in R$, and acceleration input $u_i \in R$.

The standard local voting protocol is a gradient-based control using the graph Laplace potential (1.3.1). We have seen in previous chapters that this protocol guarantees consensus if the graph has a spanning tree. Other local protocols can be derived using different potential functions, as indicated by the next exercise.

Exercise 1.3-1. Local Protocol Based on a Linear Potential Function: Finite-Time Consensus. Consider planar motion given by the velocity control dynamics (1.3.5) with $x_i = [p_i \;\; q_i]^T \in R^2$ where $(p_i(t), q_i(t))$ is the position of node i in the (x,y)-plane. Define the linear potential

$$V_G = \sum_{i,j} a_{ij} r_{ij} \tag{1.3.17}$$

where the distance between nodes i and j is given by (1.3.10). Show that the gradient-based local protocol is

$$u = -\frac{\partial V_G}{\partial x_i} = \sum_{j \in N_i} a_{ij} \frac{(x_j - x_i)}{r_{ij}} = \sum_{j \in N_i} a_{ij} \frac{(x_j - x_i)}{\left| x_j - x_i \right|} \tag{1.3.18}$$

Does this protocol guarantee consensus?

Argue that this law guarantees convergence to *consensus in finite time* regardless of the graph topology, as long as the graph has a spanning tree. We shall discuss finite-time consensus in a later chapter.

■

Note that vehicle dynamics for motion in n dimensions are actually of second order in the Newton's law form

$$\begin{aligned} \dot{x}_i &= v_i \\ \dot{v}_i &= u_i \end{aligned} \tag{1.3.19}$$

with vector position $x_i \in R^n$, speed $v_i \in R^n$, and acceleration input $u_i \in R^n$. Potential field methods can also be used to derive the acceleration controls for such systems.

1.4 Potential Field Analysis of Collective Motion

Equation Section (Next)

Many researchers have used potential fields to analyze the collective motion of flocks, herds, swarms, formations and other animal and human groups.

Gazi and Passino

Gazi and Passino [2003, 2004] considered swarms of *N* agents with the integrator dynamics with control given by

$$\dot{x}_i = \sum_{j \neq i} g(x_i - x_j), \; x_i \in R^n. \tag{1.4.1}$$

This amounts to communication over a fully connected undirected graph. Function *g(.)* is the gradient of a potential function consisting of a repulsive part and an attractive part, with a unique value δ where $g(\delta) = 0$. The example used was

$$g(y) = -y\left(a - b\exp\left(-\frac{\|y\|^2}{c}\right)\right), \tag{1.4.2}$$

which is equal to zero for $\delta = \sqrt{c\ln(b/a)}$, repulsive for $\|y\| < \delta$, and attractive for $\|y\| > \delta$. This potential function is shoiwn in Figure 1.4-1.

The following results are shown:

Define the center of the swarm as $\bar{x} = \frac{1}{N}\sum_{i=1}^{N} x_i$. Then the center is stationary, $\dot{\bar{x}} = 0$.

Let an agent *i* satisfy $\|x_i - x_j\| > \delta, \forall j \neq i$, i.e. it experiences purely attractive forces. Then its motion is towards the center. The proof uses the Lyapunov function $V_i = \frac{1}{2}(x_i - \bar{x})^T(x_i - \bar{x})$.

As time passes, the agents will converge to a hyperball $\|x - \bar{x}\| \leq \varepsilon$, with radius $\varepsilon = \frac{b}{a}\sqrt{\frac{c}{2}}\exp(-1/2)$. This is independent of the number of agents *N*, so density increases with *N*.

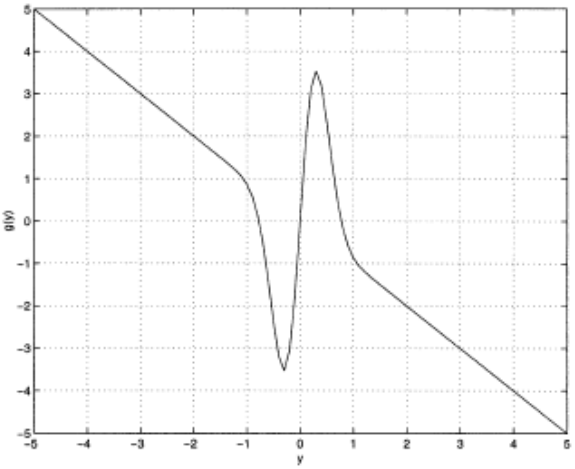


Fig. 1.4-1. Potential field function. Courtesy of (Gazi and Passino 2003).

The motion converges with time to $\dot{x} = 0$, i.e. all agents come to relative rest. The proof is based on the Lyapunov potential field function

$$V(x) = \frac{1}{2}\sum_{i=1}^{M-1}\sum_{j=i+1}^{M}\left[a\|x_i - x_j\|^2 + bc\exp\left(-\frac{\|x_i - x_j\|^2}{c}\right)\right]. \tag{1.4.3}$$

Then the gradient gives force and hence the closed-loop system.

Define the local potential function

$$V_i(x) = \tfrac{1}{2}\sum_{\substack{j=1 \\ j\neq i}}^{M} \left[a\left\|x_i - x_j\right\|^2 + bc\exp\left(-\frac{\left\|x_i - x_j\right\|^2}{c} \right) \right]. \qquad (1.4.4)$$

Then each agent minimizes its local potential function, and the global minimum is achieved.

If each agent has finite body size of radius η, then the swarm size is bounded below by $\varepsilon = \eta\sqrt[n]{N}$. Now the size depends on the number of agents. The density is now bounded above by $\rho \le 1/\pi\eta^2$.

Gazi [2005] extends the above integrator dynamics results to vehicles with Lagrangian dynamics $M_i\ddot{x}_i + f_i = u_i$ by defining the sliding manifold $s_i = \dot{x}_i + \nabla_{x_i} V(x) = 0$ with *V(x)* a potential function. On the sliding manifold one has $\dot{x}_i = -\nabla_{x_i} V(x)$ as above.

Leonard and Fiorelli

In [Leonard and Fiorelli 2001] potential field control of position/speed dynamics $\dot{p}_i = v_i, \dot{v}_i = u_i$ is considered. Define a potential function $V(r_{ij})$ with r_{ij} the distance from node *j* to node *i*. Define the gradient $f_{ij}(r_{ij}) = \nabla_{r_{ij}} V(r_{ij})$. Control is taken as

$$u_i = -\sum_{j\neq i} \frac{f_{ij}}{\left|r_{ij}\right|} r_{ij} + f_{v_i} \qquad (1.4.5)$$

with the last term a damping term, e.g. $f_{v_i} = -av_i$ or $f_{v_i} = -a\dot{p}_i$. This assumes a fully connected undirected graph communication topology.

Define polar coordinates $r_i = \begin{bmatrix} r_i\cos\theta_i \\ r_i\sin\theta_i \end{bmatrix}$. Then the closed loop system (without damping) is

$$\ddot{r}_i = \dot{r}_i\dot{\theta}_i^2 - \sum_{j\neq i}\left(r_i - r_j\cos(\theta_i - \theta_j)\right)\frac{f_{ij}(r_{ij})}{\left|r_{ij}\right|} \qquad (1.4.6)$$

$$r_i\ddot{\theta}_i = -2\dot{r}_i\dot{\theta}_i - \sum_{j\neq i} r_j\sin(\theta_i - \theta_j)\frac{f_{ij}(r_{ij})}{\left|r_{ij}\right|} \qquad (1.4.7)$$

The last equation is very similar to the Kuramoto oscillators [Strogatz, Kuramoto].

Flocking is considered. Also considered is schooling, where a desired velocity is to be followed by the swarm. Then, $f_{v_i} = a(v_d - v_i)$ with v_d the desired velocity.

Olfati-Saber and Murray

[Olfati-Saber and Murray 2004] consider the motion dynamics $\dot{p}_i = v_i, \dot{v}_i = u_i$ and graph theory is used. A flock is defined as a weakly connected digraph, or a connected undirected graph. Define the c.g. as $\overline{p} = ave(p) = \sum_i p_i$ and the relative position as $\tilde{p}_i = p_i - \overline{p}$. Then the

translational dynamics are $\dot{\bar{p}}_i = \bar{v}_i, \dot{\bar{v}}_i = \bar{u}_i$ and the relative dynamics are $\dot{\tilde{p}}_i = \tilde{v}_i, \dot{\tilde{v}}_i = \tilde{u}_i$. A separation principle is shown. The zero eigenvalue of the Laplacian matrix corresponds to the absolute motion of the c.g.

The flocking protocol used is

$$u_i = \sum_{j \in N_i} \frac{f_{ij}\left(\left\|p_j - p_i\right\| - d_{ij}\right)}{\left\|p_j - p_i\right\|}(p_j - p_i) + c_d(v_j - v_i) \tag{1.4.8}$$

or

$$u_i = \sum_{j \in N_i} s_{ij}(p_j - p_i) + c_d(v_j - v_i) \tag{1.4.9}$$

with s_{ij} the edge stress weights, d_{ij} the desired separation, and c_d the damping. The force f_{ij} is the gradient of a potential function.

Dang and Lewis [2006] used potential field methods for dynamic localization in wireless sensor networks. They defined a Lyapunov function similar to (1.3.9) in terms of an 'error potential,' and took the gradient-based control to update estimates in an observer for estimation of the positions of nodes in a network.

1.5 Potential Field Control of Nonholonomic Vehicles

Equation Section (Next)

Unicycle Vehicles

In [Lin, Francis, Maggiore 2005] unicycle agents were considered

$$\begin{aligned} \dot{x}_i &= v_i \cos\theta_i \\ \dot{y}_i &= v_i \sin\theta_i \\ \dot{\theta}_i &= \omega_i \end{aligned} \tag{1.5.1}$$

or

$$\begin{aligned} \dot{\bar{z}}_i &= v_i e^{j\theta_i} \\ \dot{\theta}_i &= \omega_i \end{aligned} \tag{1.5.2}$$

with $\bar{z}_i = x_i + jy_i$. The control is taken as

$$\begin{aligned} v_i &= k\sum_{j \in N_i}(z_j - z_i)\bullet r_i \\ \omega_i &= \cos t \end{aligned} \tag{1.5.3}$$

in terms of the dot product, with $z_i = [x_i \; y_i]^T$ and r_i the Frenet-Serret vector tangent to the trajectory. Then the closed-loop dynamics is $\dot{z} = -kH(\theta(t))\left(L \otimes I_2\right)z$ with $H(\theta(t)) = diag\{r_i r_i^T\}$ and $\otimes$ the Kronecker matrix product.

It was shown that the formation stabilizes to a point (i.e. all vehicles converge to the same value of z_i) for all initial (x_i, y_i, θ_i) if and only if the graph has a reachable node. They define graph edge arrows 'backwards,' so that agent i obtains information from agent j if there is an

edge from *i* to *j*. Therefore, in our terminology, a reachable node corresponds to existence of a node connected to all other nodes, i.e. a spanning tree.

It was shown that the formation stabilizes to a line if and only if there are at most two disjoint closed sets of nodes in the control digraph.

Nonlinear Formation Control Law.

In [Justh and Krishnaprasad 2002] are considered nonholonomic vehicle dynamics in kinematic Frenet-Serret form

$$\begin{aligned} \dot{r}_k &= x_k \\ \dot{x}_k &= y_k u_k \\ \dot{y}_k &= -x_k u_k \end{aligned} \tag{1.5.4}$$

with *r* the position and *x,y* orthogonal vectors specifying the orientation. The control law is

$$u_k = \sum_{j \neq k} \left[-\eta(|r_{jk}|) \left(\frac{r_{jk}}{|r_{jk}|} . x_k \right) \left(\frac{r_{jk}}{|r_{jk}|} . y_k \right) - f(|r_{jk}|) \left(\frac{r_{jk}}{|r_{jk}|} . y_k \right) + \mu(|r_{jk}|) x_j . y_k \right] \tag{1.5.5}$$

with $r_{kj} = r_j - r_k$ and using the dot product. It is shown using Lyapunov methods that the system converges to the equilibrium points.

In the control, the last term forces a common orientation. Using this term only yields $u_k = \mu \sum_{j \neq k}^{N} x_j . y_k$. Define $x_k = \exp(i\theta_k)$. Then $y_k = \left(i \exp(i\theta_k) \right)^*$, and this becomes $\dot{\theta}_k = u_k = \mu \sum_{j \neq k} \sin(\theta_j - \theta_k)$. This is the Kuramoto oscillator [Strogatz, Kuramoto], and is the gradient system with respect to the energy function $V_{orient} = -\frac{\mu}{2} \sum_{j,k} \cos(\theta_k - \theta_j)$.

The function *f(.)* allows one to achieve a desired separation, for it is shown that equilibrium points have $f(\rho) - \frac{1}{\rho} = 0$.

References

P. Dang, F.L. Lewis, and D.O. Popa, "Dynamic Localization of Air-Ground Wireless Sensor Networks," Proc. Mediterranean Conf. Control and Automation paper WM1-1, Ancona, June 2006.

Gazi V., Passino K.M., "Stability analysis of swarms," IEEE Trans. Automatic Control, **48**(4), 692-697 (2003).

Gazi V., Passino K.M., "Stability Analysis of Social Foraging Swarms," IEEE Trans. on Systems, Man, and Cybernetics-Part B: Cybernetics, Vol. 34, No. 1. Feb. pp. 539-557, 2004.

[Justh and Krishnaprasad 2002]

N.E. Leonard and E. Fiorelli, "Virtual leaders, artificial potentials, and coordinated control of groups," Proc. IEEE Conf. Decision and Control, pp. 2968-2973, Dec. 2001.

[Lin, Francis, Maggiore 2005]

R. Olfati-Saber and R.M. Murray, "Consensus problems in networks of agents with switching topology and time-delays," IEEE Trans. Automatic Control, vol. 49, no. 9, pp. 1520-1533, Sept. 2004.

Y. Kuramoto, *Chemical Oscillations, Waves, and Turbulence*, Springer, Berlin, 1984.

E. Stingu and F.L. Lewis, *Neuro Fuzzy Control of Autonomous Robotics*, in Encyclopedia of Complexity and Systems Science, ed. R.A. Meyers, Springer, Berlin, 2009.

S.H. Strogatz, "From Kuramoto to Crawford: exploring the onset of synchronization in populations of coupled oscillators," Physica D, vol. 143, pp. 1-20, 2000.